J Biomol NMR
DOI 10.1007/s10858-015-9905-z

ARTICLE

Optimizing nanodiscs and bicelles for solution NMR studies of two β-barrel membrane proteins

Iga Kucharska · Thomas C. Edrington · Binyong Liang · Lukas K. Tamm

Received: 21 November 2014 / Accepted: 21 January 2015

Abstract Solution NMR spectroscopy has become a robust method to determine structures and explore the dynamics of integral membrane proteins. The vast majority of previous studies on membrane proteins by solution NMR have been conducted in lipid micelles. Contrary to the lipids that form a lipid bilayer in biological membranes, micellar lipids typically contain only a single hydrocarbon chain or two chains that are too short to form a bilayer. Therefore, there is a need to explore alternative more bilayer-like media to mimic the natural environment of membrane proteins. Lipid bicelles and lipid nanodiscs have emerged as two alternative membrane mimetics that are compatible with solution NMR spectroscopy. Here, we have conducted a comprehensive comparison of the physical and spectroscopic behavior of two outer membrane proteins from *Pseudomonas aeruginosa*, OprG and OprH, in lipid micelles, bicelles, and nanodiscs of five different sizes. Bicelles stabilized with a fraction of negatively charged lipids yielded spectra of almost comparable quality as in the best micellar solutions and the secondary structures were found to be almost indistinguishable in the two environments. Of the five nanodiscs tested, nanodiscs assembled from MSP1D1ΔH5 performed the best with both proteins in terms of sample stability and spectral resolution. Even in these optimal nanodiscs some broad signals from the membrane embedded barrel were severely overlapped with sharp signals from the flexible loops making their assignments difficult. A mutant OprH that had two of the flexible loops truncated yielded very promising spectra for further structural and dynamical analysis in MSP1D1ΔH5 nanodiscs.

Keywords Solution NMR · Membrane protein · β-Barrel · Bicelle · Nanodisc

Introduction

Membrane proteins constitute around 30 % of the human genome and are the targets of many therapeutic agents (Wallin and von Heijne 1998). Despite their importance there is substantially less structural and functional data available about them compared to soluble proteins, mainly due to difficulties in the expression and purification of sufficient yields and their preparation in suitable membrane-mimicking environments. Membrane proteins are most frequently prepared in detergent micelles for structural analysis by X-ray crystallography or solution NMR. However, in some detergents membrane proteins may partially or fully denature resulting in loss of activity (Linke 2009; Tate 2010). Therefore, there is a need to find better mimics of the natural lipid bilayer membrane environment when structurally characterizing membrane proteins.

Certain mixtures of long- and short-chain phospholipids form dynamic disc-shaped assemblies called lipid bicelles (Sanders and Prestegard 1990; Sanders and Schwonek

Electronic supplementary material The online version of this article (doi:10.1007/s10858-015-9905-z) contains supplementary material, which is available to authorized users.

I. Kucharska · T. C. Edrington · B. Liang · L. K. Tamm (✉)
Center for Membrane Biology and Department of Molecular Physiology and Biological Physics, University of Virginia, Charlottesville, VA 22908, USA
e-mail: Lkt2e@virginia.edu

Present Address:
T. C. Edrington
Monsanto Company, 800 N. Lindbergh Blvd., Creve Coeur, MO 63141, USA

Published online: 10 February 2015

1992; Sanders and Prosser 1998). For studying membrane proteins by solution NMR spectroscopy they are frequently composed of one part of 1,2-dimyristoyl-*sn*-glycero-3-phosphocholine (DMPC) and two to four parts of 1,2-dihexanoyl-*sn*-glycero-3-phosphocholine (DHPC). DMPC is thought to form a central bilayered core surrounding the protein of interest while DHPC forms the edge of a disc-shaped assembly. However, this segregation is probably not very strict and both types of lipids are likely in fairly rapid dynamic exchange (Sanders and Prosser 1998). The size of lipid bicelles can be manipulated by changing the ratio of the long- to short-chain lipids, or q value, but only a relatively limited range of q values from $\sim$0.25 to 0.5 is useful for solution NMR. Successful solution NMR studies in bicelles include among others the structure determinations of the transmembrane segments of integrin β3 (Lau et al. 2008), the transporter Smr (Poget et al. 2007), the receptor tyrosine kinase EphA1 (Bocharov et al. 2008), synaptobrevin-2 (Liang et al. 2014) and the amyloid precursor protein C99 (Song et al. 2014).

A recent and very promising advance as a small-scale model of a lipid bilayer that is suitable for solution NMR studies is the development of lipid nanodiscs (Bayburt et al. 2002; Denisov et al. 2004; Gluck et al. 2009). Nanodiscs are fragments of lipid bilayers surrounded by two copies of the α-helical amphipathic apolipoprotein A-I. The presence of a defined protein belt around a small patch of lipid bilayer ensures the controlled size and monodispersity of nanodiscs, which is thought to be an important advantage of this system compared to the more heterogeneous micelle and bicelle preparations. Importantly, nanodiscs are detergent-free, and therefore, embedded membrane proteins should not be influenced by adverse detergent effects. Several membrane proteins have been successfully reconstituted into nanodiscs and studied by solution NMR, including the helical transmembrane domains of CD4 (Gluck et al. 2009), the viral proteins pf1, p7, and the G-protein-coupled receptor CXCR1 (Park et al. 2011), bacteriorhodopsin (Etzkorn et al. 2013; Hagn et al. 2013), YgaP (Tzitzilonis et al. 2013), and the β-barrel membrane proteins OmpX (Hagn et al. 2013), OmpA (Susac et al. 2014), VDAC1 (Raschle et al. 2009) and VDAC2 (Yu et al. 2012). However, the size of conventional nanodiscs is estimated to be $\sim$120 kDa before the membrane protein of interest is added, which makes 3D NMR experiments very challenging, often requiring lipid deuteration and very high-field instruments to achieve the best resolution. To partially ameliorate this problem Hagn et al. (Hagn et al. 2013) engineered shorter versions of the standard MSP1 apolipoprotein that yielded substantially smaller nanodiscs with diameters ranging from around 6 to 10 nm. The generation and use of these smaller nanodiscs was essential for obtaining very high-quality NMR spectra of OmpX, which led to solving the first structure of a membrane protein in nanodiscs.

Motivated by this work, we present a detailed comparison of membrane-mimetic conditions—using lipid micelles, bicelles and nanodiscs—to obtain spectra of good and lesser quality of two β-barrel outer membrane proteins from *P. aeruginosa*, namely OprG and OprH. Although unrelated in sequence and function, both proteins share similar topologies: they are eight-stranded β-barrels with four relatively long extracellular loops and three short periplasmic turns. OprG is speculated to function as a transporter of hydrophobic substrates through the outer membrane (Touw et al. 2010) and OprH functions to provide stability to the outer membrane of *P. aeruginosa* by directly interacting with lipopolysaccharides (LPS) in the membrane (Edrington et al. 2011).

Materials and methods

Expression and purification of OprG and OprH proteins

OprG and OprH sequences were cloned from *P. aeruginosa* PAO1 DNA into a pET30a+ vector containing the T7 promoter (EMD Biosciences, Billerica, MA). Both constructs were cloned without the N-terminal signal sequence (in OprG residues 1–26 were replaced with Met1 so that His27 becomes His2 in our numbering system; in OprH residues 1–22 were replaced with Met-1 so that Ala-23 becomes Ala-2 in our numbering system) and contained a C-terminal 6xHis-tag (Supplementary Fig. 1). ^{2}H-,^{15}N-labeled *P. aeruginosa* OprG and OprH were expressed in *E. coli* strain BL21(DE3) (Agilent Technologies, Santa Clara, CA), purified and refolded as described previously for OprH (Edrington et al. 2011).

Site-directed mutagenesis of OprH

Primers were designed to remove the loop 1 residues Ile17–Asn38 and the loop four residues Thr150–Ser162 from the OprH sequence (Supplementary Fig. 1) using the Stratagene (Santa Clara, CA) QuikChange site-directed mutagenesis kit. Parent DNA coding for wild-type (wt) OprH and the forward and reverse primers of each desired mutation were cycled 20 times in a PCR reaction where the annealing step was set to 68 °C. Amplification products were digested for 1 h with the restriction enzyme DpnI. The DNA was transformed using XL1-Blue supercompetent cells from Agilent Technologies according to manufacturer's recommended protocol. The resulting loop deletion construct (OprHΔL1ΔL4) was expressed and refolded using the same methods as wt OprH.

Expression and purification of MSP proteins

The plasmids for all membrane scaffold protein (MSP) constructs were obtained from Dr. Gerhard Wagner (Harvard Medical School). *E. coli* strain BL21(DE3) competent cells were transformed with the desired MSP plasmid. One colony from the transformation was used to inoculate 20 ml of LB media. This preculture was grown overnight at 37 °C (225 rpm shaker speed). The 20 ml preculture was pelleted at 25 °C for 10 min at 4,000 rpm and resuspended in 1 L of LB media. 1 L cultures were grown at 37 °C to an OD of 0.5. After the addition of 1 mM isopropyl β-D-1 thiogalactopyranoside (IPTG) the culture was incubated at 37 °C for 3–4 h. Cells were pelleted at 6,000 rpm and 4 °C for 15 min and stored at –80 °C or immediately purified. The cell pellets were resuspended on ice in 10 ml of 50 mM Tris/HCl pH 8.0, 500 mM NaCl, 1 mM EDTA (Buffer A) supplemented with 1 % TritonX-100 and 100 µL of Pierce (Waltham, MA) protein inhibitor cocktail. The resuspended pellets were lysed with three passes through a MP-110P microfluidizer (Microfluidics, Newton, MA) at 20,000 psi. Much of the MSP proteins were found in the insoluble fractions, depending on the expression level or the construct purified. The soluble cell fractions were separated from the insoluble inclusion bodies by centrifugation at 11,000×*g* for 15 min at 4 °C. The supernatants were stored separately and inclusion bodies were resuspended in 10 ml of Buffer A. After centrifugation at 11,000×*g* for 15 min at 4 °C the inclusion bodies were again resuspended in 10 ml of Buffer A. This washing of the inclusion bodies was repeated three times. The washed inclusion bodies were resuspended in 10 ml of 50 mM $NaPO_4$ pH 8.0, 300 mM NaCl, 8 M urea (Buffer B) and rotated at 4 °C for 2 h. The supernatant and solubilized inclusion bodies were combined with prewashed Ni–NTA agarose beads (Qiagen) and rotated separately at 4 °C for 1 h. The Ni–NTA columns were washed with 5 ml of Buffer A supplemented with 1 % TritonX-100 and combined. Beads were washed with five column volumes of Buffer A plus 50 mM sodium cholate, five column volumes of Buffer A and five column volumes of Buffer A plus 20 mM imidazole. MSPs were eluted with Buffer A plus 500 mM imidazole and 10 mM sodium cholate (addition of sodium cholate was optional, but we noticed it prevented protein precipitation during concentration). The eluted volume was concentrated to ~10 ml using Ultra15 3,000 MWCO membranes (Millipore, Billerica, MA) and loaded on a Superdex 26/60 column pre-equilibrated with 50 mM Tris pH 8, 100 mM NaCl, 4 mM β-mercaptoethanol (Buffer C). Fractions containing the proteins were pooled and concentrated to ~10 ml.

TEV cleavage

Tobacco etch virus protease (purified following the protocol of (Tropea et al. 2009)) was added to the purified MSP protein solutions (1 A_{280} unit of TEV for 100 A_{280} units of MSP protein) and incubated overnight at 4 °C. The supernatants were rotated at 4 °C for 1 h with prewashed (Buffer C) Ni–NTA agarose beads. The beads were washed with Buffer C until MSPs were no longer detectable in the wash. The flow-through and wash fractions containing proteins were pooled and 10 mM sodium cholate and 2 mM EDTA were added to the protein solutions. The proteins were concentrated to 5–10 mg/ml, flash frozen in liquid N_2 and stored at −80 °C. The nomenclature adopted here and similarly elsewhere (Hagn et al. 2013; Schuler et al. 2013) designates MSPs with cleaved N-terminal His-tags MSP1D1(Δx) and those with uncleaved N-termini MSP1(Δx).

Nanodisc assembly

Nanodiscs were assembled following established protocols (Denisov et al. 2004; Ritchie et al. 2009; Hagn et al. 2013). DMPC solubilized in sodium cholate (at 2:1 cholate/DMPC ratio), MSP and OprG or OprH were mixed in MSP buffer (20 mM Tris/HCl pH 7.5, 100 mM NaCl, 5 mM EDTA, 0.01 % sodium azide) at a ratio of 60 µM OprG or OprH to 240 µM MSP. The MSP-to-lipid ratios were 1:65, 1:40, and 1:20 for MSP1D1, MSP1D1ΔH4 or ΔH5, and MSP1D1ΔH4ΔH5 or MSP1D1ΔH4-ΔH6, respectively, as proposed for the similarly-sized protein OmpX (Hagn et al. 2013). After incubation at 4 °C for 2 h, 1–1.5 g of wetted Biobeads SM-2 (Biorad, Hercules, CA) were added per 1 ml of the assembly mixture and the suspension was rotated overnight at room temperature. The assembly mixture with Bio-Beads was applied on a gravity column and washed with 1× volume MSP buffer. Since OprH and OprG contain C-terminal 6xHis-tags, it is possible to separate empty from OprH- or OprG-containing nanodiscs by binding the particles to Ni–NTA beads. The flow through and washes from the Bio-Beads were combined and mixed with prewashed Ni–NTA beads and incubated with mixing for 1 h at 4 °C and applied to a gravity column. The flow throughs were discarded and the OprH- or OprG-containing nanodiscs were eluted with MSP buffer plus 300 mM imidazole. The eluate was concentrated to ~0.5 ml using an Amicon centrifugal unit of 10 kDa MWCO (Millipore), filtered and loaded on a Superdex 200 10/30 size exclusion column that was equilibrated with 20 mM sodium phosphate pH 6.5, 50 mM KCl, 1 mM EDTA, 0.01 % sodium azide. Fractions containing OprH or OprG nanodiscs were combined and concentrated using an Amicon centrifugal unit of 10 kDa MWCO. The final

NMR samples contained ~0.5 mM of $^{2}H,^{15}N$-labeled OprG or OprH.

Preparation of q = 0.3 bicelles composed of DHPC:DMPC:DHPS:DMPS 27:9:3:1

All lipids were purchased from Avanti Polar Lipids (Alabaster, AL) or Anatrace (Maumee, OH). Bicelles were prepared according to the established protocols (Sanders and Schwonek 1992; Losonczi and Prestegard 1998; Struppe et al. 1998; Ellena et al. 2003). DHPC concentrations in refolded ^{2}H-,^{13}C-,^{15}N-labeled OprG and OprH samples were measured by ^{1}H-NMR with sodium 2,2-dimethyl-2-silapentane-5-sulfonate (DSS) as a standard. Appropriate amounts of solid 1,2-dihexanoyl-*sn*-glycero-3-phospho-L-serine (DHPS) were added to the protein samples and left for an hour at room temperature. The protein sample in DHPC/DHPS was added to a glass vial containing appropriate amounts of a nitrogen-dried DMPC and 1,2-dimyristoyl-*sn*-glycero-3-phospho-L-serine (DMPS) mixture. To solubilize and equilibrate the lipids, the whole protein/detergent/lipid mixture was frozen and thawed 3 times (cycles of 40 min on ice and 40 min at 40 °C).

NMR spectroscopy

All NMR experiments were recorded at 45 °C on a Bruker Avance III 800 spectrometer equipped with a triple-resonance cryoprobe. The 1D TRACT pulse scheme was used to determine rotational correlation times (Lee et al. 2006). Experiments were performed using the Bruker Topspin version 2.1.6 software suite. Sequential backbone assignments for ^{2}H-,^{13}C-,^{15}N-labeled OprH in bicelles were obtained by recording TROSY versions of HNCA, HNCB, HNCO and HNCACO experiments. The NMR data were processed with NMRPipe (Delaglio et al. 1995) and analyzed using Sparky (Goddard and Kneller).

Results

Protein expression and purification

To examine the effect of decreasing the size of nanodiscs on the quality of the NMR spectra of incorporated membrane proteins, deletion mutants of the standard membrane scaffold protein MSP1D1 (Denisov et al. 2004) were overexpressed in *E. coli* following the protocol of Hagn et al. (Hagn et al. 2013). All proteins showed good levels of expression (Fig. 1). However, we encountered some problems during their purification, which included occasional precipitation and degradation of some of the proteins. Therefore, we

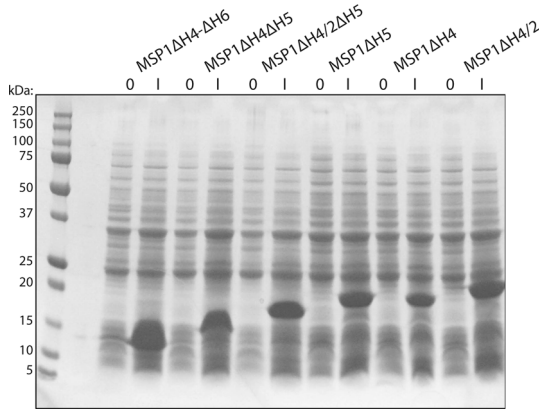

Fig. 1 Expression of different MSP constructs. SDS-PAGE of samples of BL21 cells transformed with MSP constructs before (O) and 3 h after induction with IPTG (I)

modified the original protocol and used gel filtration rather than dialysis after affinity chromatography, which in our hands resulted in shorter times for purification, higher purities, and better protein stability (Supplementary Fig. 2). We also found that the shortened mutants of MSP1D1 tended to precipitate during concentration, but the addition of cholate remedied this problem and stabilized the proteins. The OprG and OprH outer membrane proteins were overexpressed in *E. coli* with C-terminal His-tags and with their signal sequences deleted (Supplementary Fig. 1). Both proteins were expressed into inclusion bodies in high yields and solubilized in urea before being purified by Ni^{2+} affinity chromatography. Purified proteins were then refolded into DHPC micelles for further use.

Assembly of Pseudomonas outer membrane proteins in nanodiscs

We assembled OprG and OprH nanodiscs using the most stable and promising MSP constructs MSP1D1, MSP1D1ΔH4, MSP1D1ΔH5, MSP1D1ΔH4ΔH5 and MSP1D1ΔH4-ΔH6. The designation ΔHx means that helix x has been deleted from the ten-helix segmented parent sequence MSP1D1. Assembled nanodiscs were purified by size exclusion chromatography and the resulting fractions were analyzed by SDS-PAGE (Fig. 2). The gel filtration elution profiles of the MSP1D1ΔH4-ΔH6 nanodiscs (Fig. 2e, f) indicate formation of larger assemblies, which has also been observed by Hagn et al. (Hagn et al. 2013) with these smallest nanodiscs containing the *E. coli* protein OmpX. Surprisingly, the size exclusion profile of OprG_MSP1D1ΔH5 (Fig. 2c) also suggests that some nanodiscs may self-associate, but this behavior was not observed in case of OprH_MSP1D1ΔH5 nanodiscs (Fig. 2d). Thus, the behavior of the introduced membrane protein matters on how a given species of nanodiscs

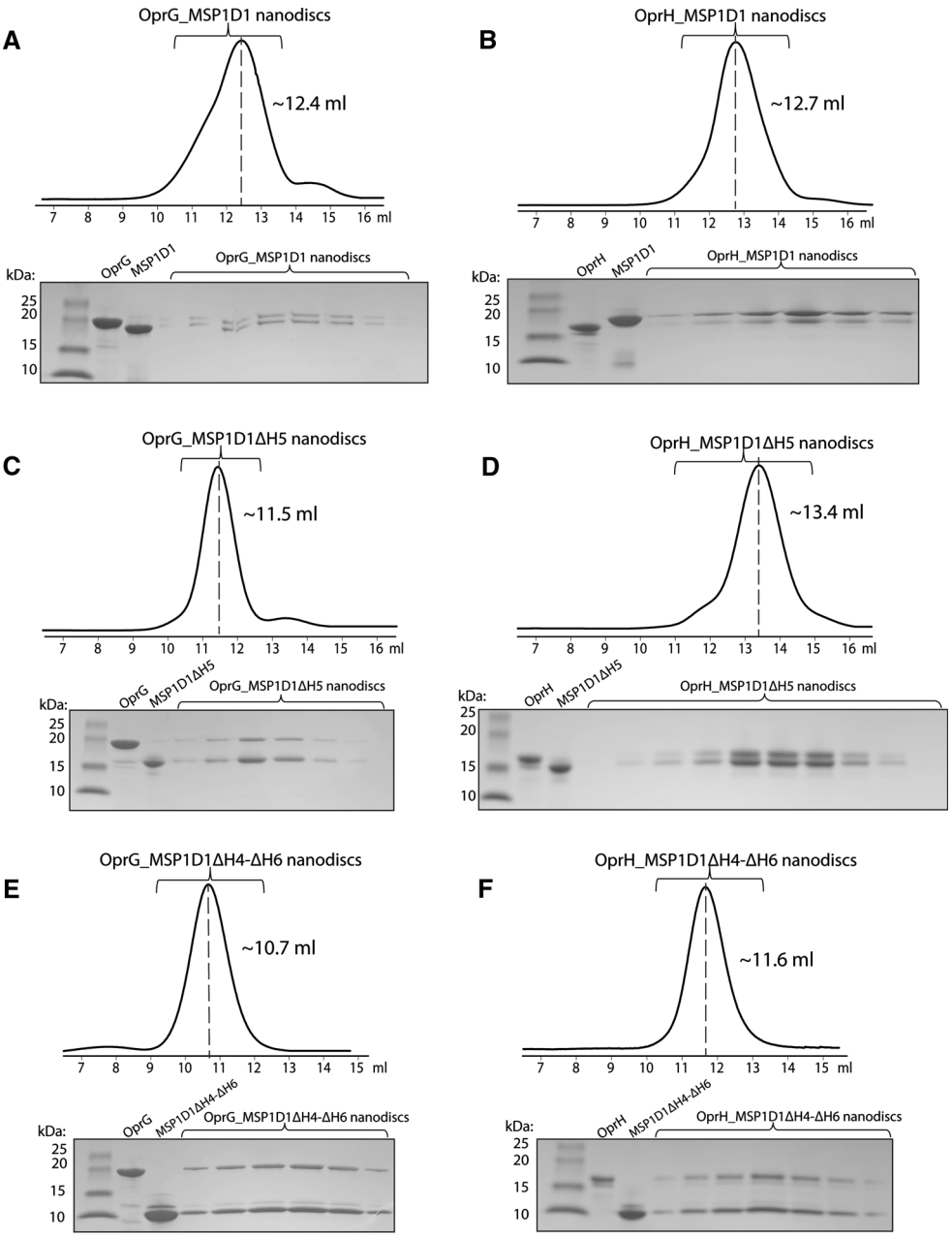

Fig. 2 Purification of reconstituted OprG-MSP and OprH-MSP nanodiscs by size exclusion chromatography. **a** OprG_MSP1D1, **b** OprH_MSP1D1, **c** OprG-_MSP1D1ΔH5, **d** OprH_MSP1D1ΔH5, **e** OprG_MSP1D1ΔH4-ΔH6, **f** OprH_MSP1D1ΔH4-ΔH6. Each *panel* shows a chromatogram on *top* and an SDS-PAGE gel of the collected fractions (*brackets*) of the reconstituted membrane protein nanodiscs and the respective individual purified protein references

behaves. In unrelated work we found that OprG has a tendency to oligomerize (unpublished results), i.e. a behavior that did not occur with OprH. Further optimization of the MSP:lipid ratios may alleviate some of these problems. An SDS-PAGE profile of the final reconstituted OprG and OprH nanodisc samples that were used for NMR experiments is shown in Fig. 3.

NMR spectroscopy of OprG and OprH in nanodiscs of various sizes

After extensive detergent screening with both OprG and OprH, DHPC proved to be optimal for the stability and NMR spectral quality of both proteins [(Edrington et al. 2011) and unpublished results]. Therefore, we use spectra of the proteins in DHPC as references to compare the spectral qualities of these proteins in nanodiscs and bicelles. The ^{1}H–^{15}N-TROSY spectrum of OprG in DHPC micelles (Fig. 4a) shows good chemical shift dispersion with some peak overlaps in the ^{1}H dimension between 7.7 and 8.6 ppm (Fig. 4a). For OprH in DHPC micelles the entire ^{1}H–^{15}N-TROSY spectrum is very well resolved (Fig. 5a) and, except for the flexible loop 1, could be almost completely assigned (Edrington et al. 2011). We collected ^{1}H–^{15}N-TROSY spectra of OprG and OprH containing nanodiscs assembled from DMPC and

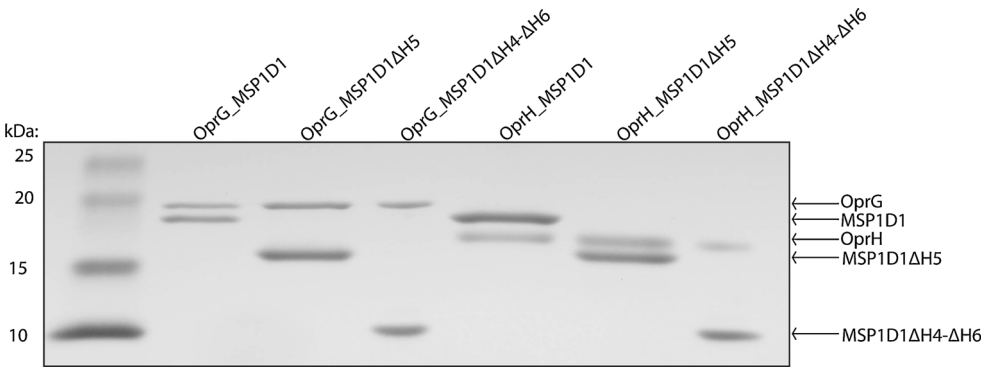

Fig. 3 SDS-PAGE of final OprG-MSP and OprH-MSP nanodisc samples. *Lane 1* protein standards, *lane 2* OprG_MSP1D1, *lane 3* OprG_ MSP1D1ΔH5, *lane 4* OprG_ MSP1D1ΔH4-ΔH6, *lane 5* OprH_MSP1D1, *lane 6* OprH_ MSP1D1ΔH5, and *lane 7* OprH_ MSP1D1ΔH4-ΔH6

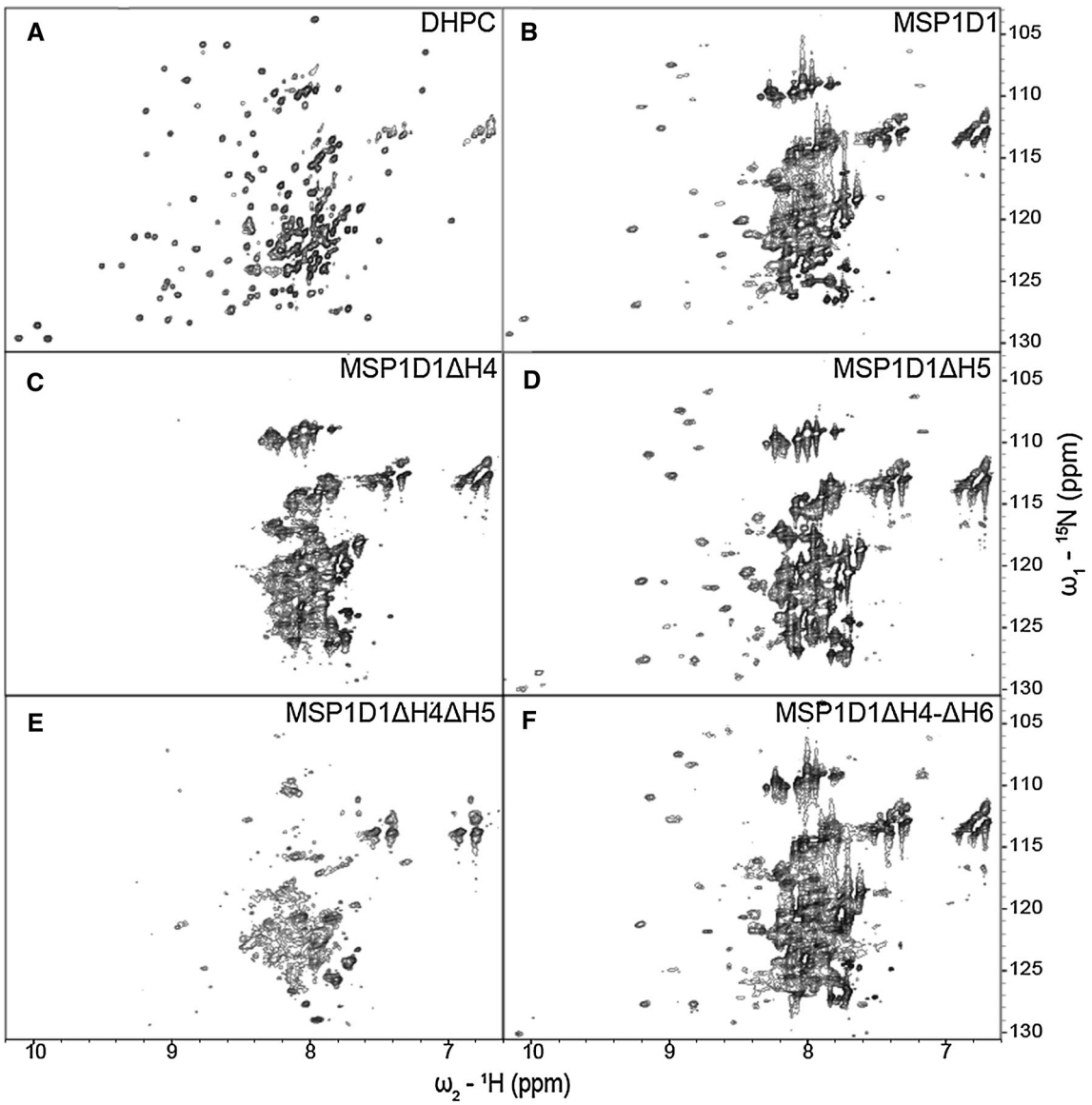

Fig. 4 ^{15}N–^{1}H TROSY spectra of ^{2}H-,^{15}N-labeled OprG in DHPC micelles and in MSP nanodiscs of *different sizes*. The OprG samples are in **a** DHPC micelles, **b** MSP1D1, **c** MSP1D1ΔH4, **d** MSP1D1ΔH5, **e** MSP1D1ΔH4ΔH5, and **f** MSP1D1ΔH4-ΔH6. All spectra were collected at 800 MHz and 45 °C

MSP1D1, MSP1D1ΔH4, MSP1D1ΔH5, MSP1D1ΔH4ΔH5 and MSP1D1ΔH4-ΔH6 (Figs. 4b–f, 5b–f, for OprG and OprH, respectively). We also assembled nanodiscs with uncut 6xHis-MSP proteins, but that resulted in nanodiscs with lower stability and reduced ^{1}H–^{15}N-TROSY spectral quality for even those MSPs that behaved well with the cut His-tags (Supplementary Fig. 3). In a few cases, we also assembled nanodiscs using a mixture of DMPC and DMPG (1,2-dimyristoyl-*sn*-glycero-3-phospho-(1′-rac-glycerol)) at a ratio 3:1 (data not shown). We did not observe an improvement of the spectral quality over nanodiscs assembled with just DMPC. Nanodiscs assembled from MSP1D1ΔH4 and MSP1D1ΔH4ΔH5 containing OprG or OprH proved to be unstable and partially precipitated during sample preparation and NMR data collection. ^{1}H–^{15}N-TROSY spectral qualities were intermediate for both outer membrane proteins when they were reconstituted in the relatively large MSP1D1 parent nanodiscs (Figs. 4b, 5b). MSP1D1ΔH5 and MSP1D1ΔH4-ΔH6 DMPC nanodiscs provided the best quality ^{1}H–^{15}N-TROSY spectra in the case of OprG (Fig. 4d, f) and OprH (Fig. 5d, f). However, even in the best quality nanodiscs the cross-peak intensities of the ^{1}H–^{15}N-TROSY spectra were not homogenous and only ~70 % of all cross-peaks that were observable in DHPC micelles could be detected (Table 1). Especially in case of OprG, broad cross-peaks in

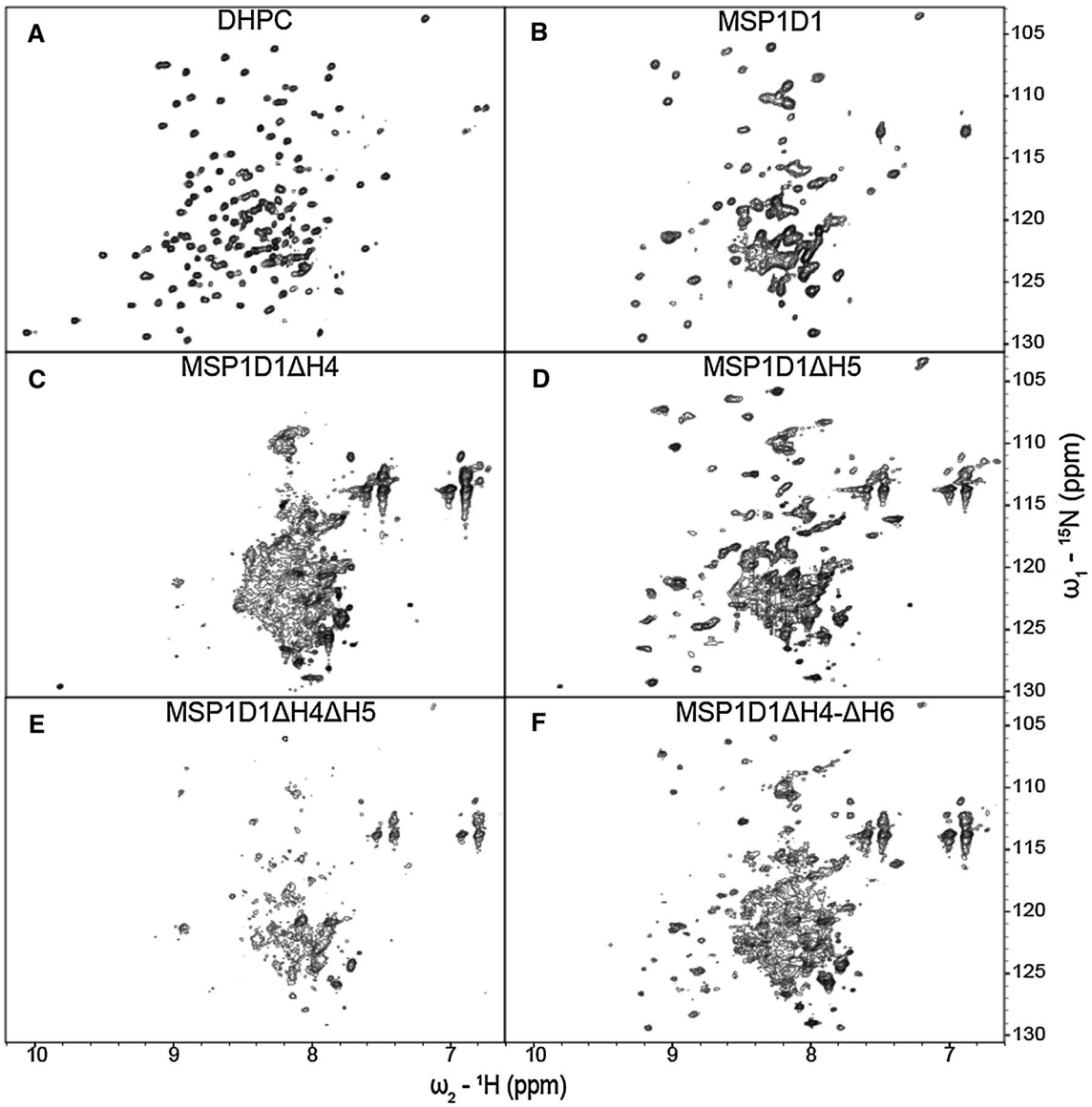

Fig. 5 ^{15}N–^{1}H TROSY spectra of ^{2}H–,^{15}N-labeled OprH in DHPC micelles and in MSP nanodiscs of *different sizes*. The OprH samples are in **a** DHPC micelles, **b** MSP1D1, **c** MSP1D1ΔH4, **d** MSP1D1ΔH5, **e** MSP1D1ΔH4ΔH5, and **f** MSP1D1ΔH4-ΔH6. All spectra were collected at 800 MHz and 45 °C

the 7.6–8.4 ppm ^{1}H region dominate over the weaker peaks in 8.4–9.4 ppm ^{1}H region. This behavior suggests that the protruding extracellular loops tumble independently from the well-ordered nanodisc-embedded β-barrel region of the protein. The summary in Table 1 shows that 45 ^{1}H–^{15}N-TROSY cross-peaks were resolved for OprG in MSP1D1ΔH5 nanodiscs and 52 cross-peaks were resolved for OprG in MSP1D1ΔH4-ΔH6 nanodiscs when the 7.6–8.4 ppm ^{1}H region was excluded from analysis due to severe peak overlap. For OprH nanodiscs we counted 60 cross-peaks in MSP1D1ΔH5 and in MSP1D1ΔH4-ΔH6 nanodiscs when the 7.75–8.35 ppm ^{1}H region was excluded. Even though MSP1D1ΔH5 nanodiscs provided better overall quality spectra than MSP1D1ΔH4-ΔH6, several additional cross-peaks were identified in the OprG_MSP1D1ΔH4-ΔH6 sample, which albeit weak could be mapped on the cross-peaks present in the spectrum of OprG in DHPC micelles.

Since the presence of the long unstructured loop regions of both proteins appears to be responsible for the observed inhomogeneous cross-peak intensities, we prepared an OprH variant, in which we removed the two longest loops. The loop 1 and loop 4 deletion mutant named OprHΔL1ΔL4 showed ^{1}H–^{15}N-TROSY spectra of excellent quality in DHPC micelles (Fig. 6a) and of good quality in MSP1D1ΔH5 nanodiscs (Fig. 6b), while its spectral quality in MSP1D1ΔH4-ΔH6 nanodiscs was more mediocre (Fig. 6c). Of the 131 cross-peaks present in the ^{1}H–^{15}N-TROSY spectra in DHPC micelles, 88 were present in MSP1D1ΔH5 nanodisc sample (Table 1). Further

Table 1 Number of resolved cross-peaks in the ordered regions of ^{15}N–^{1}H TROSY spectra of the three proteins in DHPC micelles, q = 0.3 PS-stabilized bicelles, and MSP nanodiscs of different sizes

	Number of cross-peaks in >8.4 ppm,<7.6 ppm ^{1}H region	Percentage of cross-peaks in >8.4 ppm, <7.6 ppm ^{1}H region relative to OprG in DHPC micelles (%)
OprG		
OprG DHPC micelles	76	100
OprG q = 0.3 bicelles	74	97
OprG_MSP1D1	36	47
OprG_HIS-MSP1	12	16
OprG_MSP1D1ΔH4	10	13
OprG_HIS-MSP1ΔH4	14	18
OprG_MSP1D1ΔH5	45	59
OprG_HIS-MSP1ΔH5	29	38
OprG_MSP1D1ΔH4ΔH5	16	21
OprG_MSP1D1ΔH4-Δ6	52	68
	Number of cross-peaks in >8.35 ppm, <7.75 ppm ^{1}H region	Percentage of cross-peaks in >8.35 ppm, <7.75 ppm ^{1}H region relative to OprH in DHPC micelles (%)
OprH		
OprH DHPC micelles	87	100
OprH q = 0.3 bicelles	87	100
OprH_MSP1D1	43	57
OprH_MSP1D1ΔH4	11	13
OprH_MSP1D1ΔH5	60	69
OprH_MSP1D1ΔH4ΔH5	10	12
OprH_MSP1D1ΔH4-Δ6	60	69
	Number of cross-peaks in 6.5–10.3 ppm ^{1}H region	Percentage of cross-peaks in 6.5–10.3 ppm ^{1}H region relative to OprHΔL1ΔL4 in DHPC micelles
OprHΔL1ΔL4		
OprHΔL1ΔΔL4 DHPC micelles	131	100
OprHΔL1ΔL4_MSP1D1ΔH5	88	67
OprHΔL1ΔL4_MSP1D1ΔH4-Δ6	78	60

improvement to the quality of these spectra might be achieved by including deuterated instead of protonated DMPC in the nanodiscs. We tried to measure the apparent correlation time of OprH and OprG proteins in nanodiscs of various sizes by performing 1D TRACT experiment (Lee et al. 2006). However, as OprH and OprG spectra are dominated by strong loop resonances, the obtained correlation time values did not reflect the correlation time of the tumbling particle. Only in case of OprHΔL1ΔL4 in MSP1D1ΔH5 nanodiscs were we successful in measuring a correlation time of 32 ns (Supplementary Fig. 4a), which corresponds to a particle molecular mass of ~100 kDa.

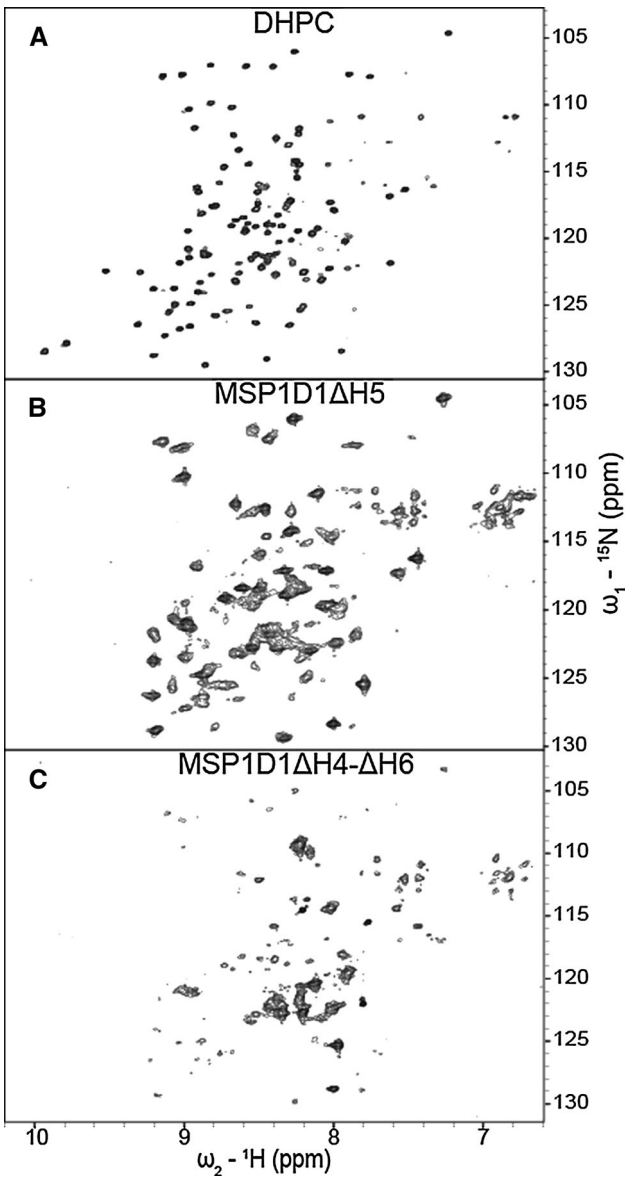

Fig. 6 ^{15}N–^{1}H TROSY spectra of ^{2}H-,^{15}N-labeled OprHΔL1ΔL4 in DHPC micelles and in MSP nanodiscs of *different sizes*. The OprHΔL1ΔL4 samples are in **a** DHPC micelles, **b** MSP1D1ΔH5, and **c** MSP1D1ΔH4-ΔH6. All spectra were collected at 800 MHz and 45 °C

NMR spectroscopy of OprG and OprH in lipid bicelles

Since lipid bicelles are also frequently used as alternatives to micelles in studies of membrane proteins by solution NMR, we wanted to compare the spectral qualities in bicelles with those of the same proteins in micelles and nanodiscs. Initial experiments of OprG and OprH in the most typical q = 0.3 DHPC:DMPC bicelles indicated that these samples had tendency to aggregate over time. Therefore, we attempted to stabilize them by doping the bicelles with 10 % of the equivalent chain-length negatively charged lipids DHPS and DMPS lipids leading to overall molar ratios of 27:9:3:1 of DHPC:DMPC:DHPS:DMPS. The rational for this approach was that the negatively charged particles would repel one another and thus prevent deleterious aggregation of the particles. Indeed, this approach allowed us to prepare high quality samples with both proteins that were stable over periods of several months.

To confirm the proper formation of OprH bicelles, we performed a 1D TRACT experiment (Supplementary Fig. 4b). The overall correlation time of the OprH in q = 0.3 PS-stabilized bicelles at 42 °C was determined to be 37 ns, which is significantly larger than 22 ns determined for OprH in DHPC micelles (Edrington et al. 2011). A correlation time of 37 ns corresponds to a protein-lipid bicelle complex of ~100 kDa with a composition of 1, 4, 12, 36 and 108 molecules of OprH, DMPS, DHPS, DMPC and DHPC, respectively. For comparison, OprH in DHPC micelles had an estimated molecular mass of 60–65 kDa (Edrington et al. 2011). A TRACT experiment performed with OprG bicelles was dominated by the flexible loops and produced an apparent correlation time of only 7 ns (Supplementary Fig. 4c). ^{1}H–^{15}N-TROSY spectra of ^{2}H,^{13}C,^{15}N-labeled OprG and OprH PS-stabilized bicelle samples (Fig. 7) showed good chemical shift dispersion and exhibited approximately the same number of cross-peaks as their respective counterparts in DHPC micelles (Table 1). This result encouraged us to collect triple-resonance NMR experiments for a de novo assignment of OprH in q = 0.3 bicelles.

TROSY versions of HNCA, HNCB, HNCO and HNCACO experiments were performed to assign HN, N, Cα, Cβ, and CO resonances of ^{2}H,^{13}C,^{15}N-OprH in q = 0.3 PS-stabilized bicelles. 139 of 180 residues (excluding the lead methionine and 6xHis-tag) could be completely assigned which is only 17 residues fewer than the 156 residues assigned in DHPC micelles (Edrington et al. 2011). The resonances of these 17 residues were more broadened or their assignments were more ambiguous in

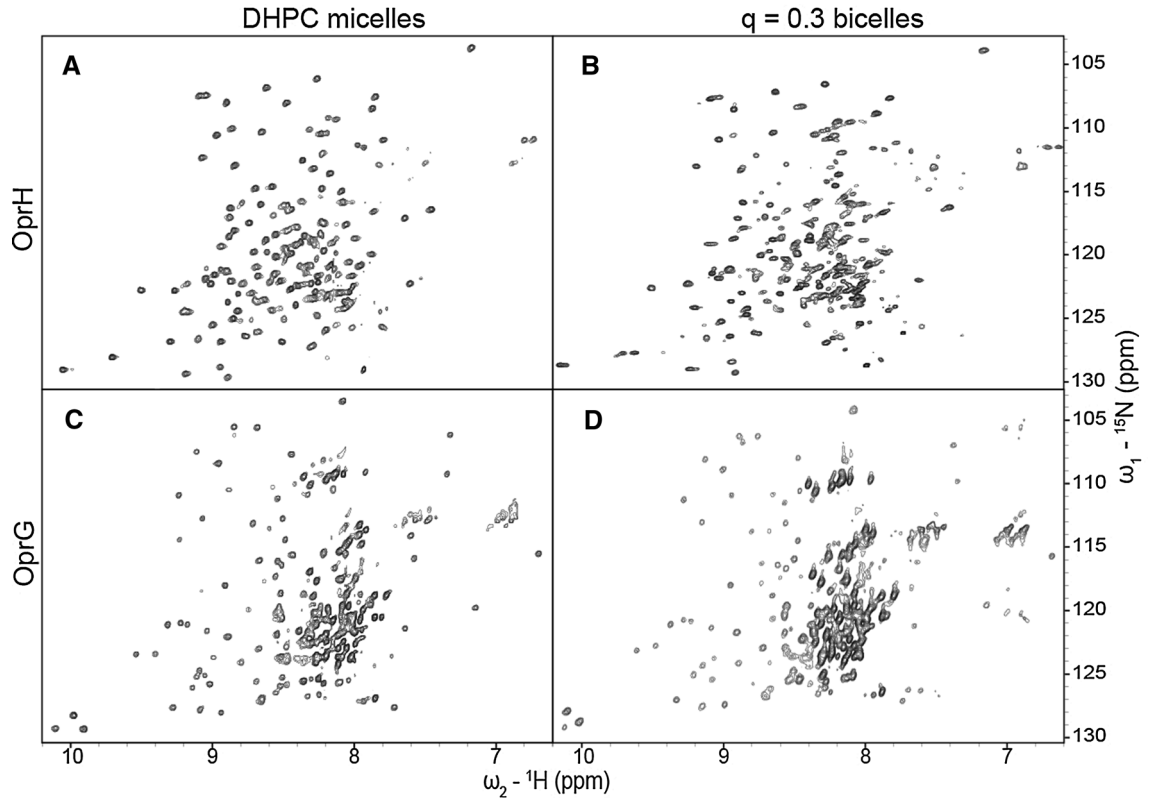

Fig. 7 ^{15}N–^{1}H TROSY spectra of ^{2}H-,^{13}C-, ^{15}N-labeled OprH (**a** and **b**) and OprG (**c** and **d**) in DHPC micelles (**a** and **c**) and in q = 0.3 DHPC:DMPC:DHPS:DMPS (27:9:3:1) bicelles (**b** and **d**). All spectra were collected at 800 MHz and 45 °C

the bicelle than in the micelle samples. Figure 8a shows the local secondary chemical shifts calculated from the Cα and Cβ chemical shifts of OprH in bicelles (Metzler et al. 1993). The secondary chemical shifts of OprH are sensitive to the presence and type of secondary structure with large negative values indicating β-strands. There are eight distinct regions of large negative values characteristic of β-strands with shorter breaks of values around zero, typical for turns or random coils. The overall topology and the limits of well-defined β-structures of the protein were virtually the same for OprH in DHPC micelles and q = 0.3 PS-stabilized bicelles [compare Fig. 8a with 4 in (Edrington et al. 2011)]. Although longer chain lipids are present in the bicelles, this did not extend the lengths of the β-strands.

We also calculated the compound NH and N chemical shift differences $\Delta\delta_{\mathrm{comp}} = \left[\Delta\delta_{\mathrm{HN}}^2 + (\Delta\delta_{\mathrm{N}}/6.5)^2\right]^{1/2}$ (Mulder et al. 1999) between ^{2}H,^{15}N,^{13}C-labeled OprH in micelles and q = 0.3 bicelles (Fig. 8b). Most residues showed no significant chemical shifts differences, but there were some notable exceptions. Significant differences were observed for residues 37, 38, 40 and 42 on β-strand 2, residues 136–138 on β-strand 7, residues 171, 173, 175 and 176 on β-strand 8, and residues 86 and 87 on periplasmic turn 2. Other minor chemical shift differences were localized in the neighborhood of the more significant ones and a very few minor changes occurred on some isolated extracellular loop residues. These chemical shift differences are mapped in Fig. 8c in a graded color scheme onto the lowest-energy conformer of the previously determined structure of OprH (Edrington et al. 2011). From an inspection of this figure it is apparent that more changes occur on the front side (left panel) than on the back side (right panel) of the β-barrel and an abundance of changes are located near the two membrane-interfacial rims of the β-barrel.

Discussion

Structural studies of integral membrane proteins require a membrane-mimetic environment that supports their correct fold and activity. In this work we have compiled a detailed comparison of the quality of solution NMR spectra of two β-barrel membrane proteins, OprG and OprH from *P. aeruginosa,* in different lipidic environments: DHPC micelles, DHPC:DMPC:DHPS:DMPS bicelles and five different DMPC nanodiscs of varied sizes. Lipid micelles are most commonly used in solution NMR of integral membrane proteins. They form relatively small particles,

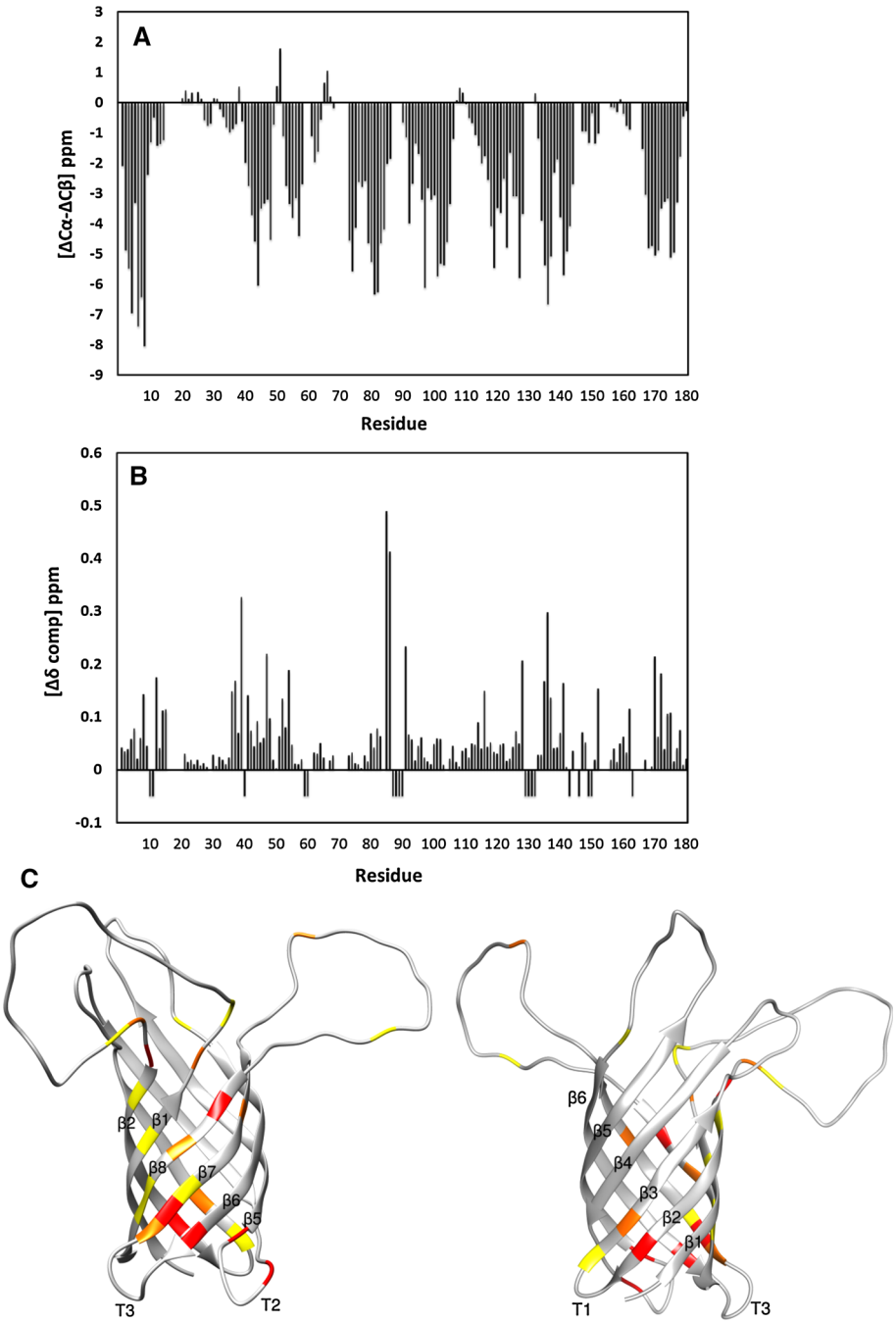

Fig. 8 Chemical shift differences between OprH in DHPC micelles and q = 0.3 DHPC:DMPC:DHPS:DMPS (27:9:3:1) bicelles. **a** Three-bond averaged ^{13}C secondary chemical shifts of ^{2}H-,^{15}N-,^{13}C-labeled OprH in q = 0.3 DHPC:DMPC:DHPS:DMPS (27:9:3:1) bicelles. **b** Compound chemical shift differences ($\Delta\delta_{comp} = \left[\Delta\delta_{HN}^2 + (\Delta\delta_N/6.5)^2\right]^{1/2}$) (Mulder et al. 1999) between ^{2}H,^{15}N,^{13}C-labeled OprH in micelles and q = 0.3 bicelles. *Negative values* indicate OprH residues unassigned in q = 0.3 bicelles. **c** The compound *chemical shift differences* of (**b**) are mapped onto the lowest-energy conformer of OprH in DHPC micelles (PDB code: 2LHF). Increasing chemical shift changes are depicted with increasingly more *red* colors. *Yellow*, *orange*, and *red* depict Δδ changes of 0.1–0.15, 0.15–0.2, and more than 0.2 ppm, respectively. The largest chemical shift perturbations occur near the interfacial regions of the β-strands and on the front face (*left*) rather than on the back face (*right*) of the β-barrel

typically on the order of 40–60 kDa for the most successfully used amphiphiles with membrane proteins on the order of 20–25 kDa that have yielded well-resolved solution NMR spectra. In many cases, including the case of OprH (Edrington et al. 2011), structures of such micelle-embedded membrane protein samples could be solved.

Small q ("isotropic") bicelles form particles that are substantially larger (80–120 kDa including a ~20–25 kDa membrane protein) and therefore are more challenging for structural studies by solution NMR. The obvious advantage of bicelles is that they contain long-chain lipids such as DMPC that on their own form lipid bilayers and thus may provide a more natural environment for embedded membrane proteins. For the cases of OprG and OprH in the current study we estimate that about 40 long-chain lipids (DMPC and DMPS) were present in the sample for each molecule of protein, which is sufficient to surround the perimeters of these β-barrel proteins by a complete double layer of long-chain lipids. However, about 120 short-chain lipids per protein were also present in these samples. These short-chain lipids are most likely in rapid exchange with the long-chain lipids (Sanders and Prosser 1998). Therefore, the membrane proteins likely experience transient interactions not only with the long-chain, but also with the short-chain lipids and their structures may hence be influenced by both types of lipids.

Lipid nanodiscs most closely approach the situation of a membrane protein in a native phospholipid bilayer. They are detergent-free, contain different amounts (depending on their size) of bilayered long-chain lipids, and are delimited by a belt formed by two copies of an amphipathic MSP. The parent scaffold protein MSP1D1 contains 189 residues that are organized into ten amphipathic α-helical segments of variable lengths. MSP1D1 nanodiscs are about 10 nm in diameter and contain about 160 molecules of DMPC plus two copies of MSP1D1. Their molecular mass without an incorporated integral membrane protein is around 130 kDa or around 160 kDa when a ~25 kDa integral protein is included (Hagn et al. 2013), making them significantly more challenging than "isotropic" bicelles for solution NMR studies of included membrane proteins. MSP1D1ΔH5 and MSP1D1ΔH4 nanodiscs contain about 100 and 90 molecules of DMPC, respectively, are about 8 nm wide, and have empty molecular masses of ~90 kDa. The even smaller nanodiscs MSP1D1ΔH4ΔH5 and MSP1D1ΔH4-ΔH6 contain about 40 and 20 molecules of DMPC, are about 7 and 6 nm wide, and have empty molecular masses of ~70 and ~50 kDa, respectively. However, the very smallest MSP1D1ΔH4-ΔH6 nanodiscs, when not hosting an integral membrane protein, were not stable over time and appeared to be in equilibrium with larger particles as also reported by Hagn et al. (Hagn et al. 2013).

Different sizes of nanodiscs presented here influence the size of the host protein that can be accommodated. MSP1D1ΔH4ΔH5 and MSP1D1ΔH4-ΔH6 might be most useful for membrane-anchored proteins and single-transmembrane helices, MSP1D1ΔH5 and MSP1D1ΔH4 can be used with proteins up to ~30 kDa, for larger membrane proteins or membrane protein multimers it is advised to use MSP1D1 or even larger MSP versions like MSP2 (Hagn et al. 2013; Schuler et al. 2013).

Hagn et al. and Susak et al. performed detailed solution NMR studies on the 18 kDa membrane protein OmpX in MSP1D1ΔH5 and the 19 kDa transmembrane domain of OmpA in MSP1D1 nanodiscs, respectively (Hagn et al. 2013; Susac et al. 2014). Since it is not a priori clear which MSP would be best for other membrane proteins, we screened the 23 and 21 kDa β-barrel membrane proteins OprG and OprH from *P. aeruginosa* with five different MSPs. Nanodiscs formed from MSP1D1ΔH5 and DMPC clearly provided the best stability and best $^{1}H–^{15}N$ TROSY spectral quality for both OprG and OprH. Although this MSP has only one of the central 22-residue helical segments removed from the 189-residue parent MSP1D1 protein, the diameter of MSP1D1ΔH5 nanodiscs is 1 nm less than that of MSP1D1 nanodiscs and the molecular mass of MSP1D1ΔH5 nanodiscs is only about 70 % that of MSP1D1. Based on the 1D TRACT result we obtained for OprHΔL1ΔL4 in MSP1D1ΔH5 nanodiscs, we estimate the molecular mass of OprH_MSP1D1ΔH5 nanodiscs to be around 105 kDa and to contain about 70 molecules of DMPC arranged in a bilayer configuration around OprH. This number of lipids is sufficient to form a single continuous boundary lipid layer around the integrated membrane protein. Somewhat surprisingly, the very similarly sized nanodiscs formed from MSP1D1ΔH4 and DMPC were much less stable and performed much poorer in recorded $^{1}H–^{15}N$ TROSY spectra with OprG and OprH. Recalling the similar behavior of OmpX in MSP1D1ΔH4 nanodiscs (Hagn et al. 2013), it is apparent that these nanodiscs are, for unknown reasons, inferior to their equally sized sister MSP1D1ΔH5 nanodiscs. Hagn et al. also found MSP1D1ΔH5 to be the best scaffold protein for their spectroscopic studies of OmpX in nanodiscs (Hagn et al. 2013). The quality of their spectra permitted them to determine the structure of OmpX in MSP1D1ΔH5 nanodiscs.

The second best MSP with OprG and OprH was MSP1D1ΔH4-ΔH6, which had three 22-residue helical segments removed from MSP1D1 and which behaved more poorly with OmpX (Hagn et al. 2013). Although OprG and OprH reconstituted into the very small MSP1D1ΔH4-ΔH6 nanodiscs showed initial promise, they had the unfortunate tendency to oligomerize in experiments requiring longer times for data collection. The second smallest nanodiscs MSP1D1ΔH4ΔH5 with two central 22-residue helical segments removed from the parent MSP1D1 scaffold protein performed poorly with all three outer membrane proteins, OmpX, OprG, and OprH.

Even when the best nanodisc-forming MSP1D1ΔH5 was used, $^{1}H–^{15}N$ TROSY spectra of OprG and OprH were characterized by broad linewidths and inhomogeneous peak

intensities compared to spectra recorded in DHPC micelles. The broader linewidths are not surprising given the relatively large sizes of the nanodiscs. The inhomogeneous peak intensities can be explained by slow rotational correlation times of the nanodiscs and comparatively faster fluctuations of the long unstructured loops. Removing the two major loops from OprH in OprHΔL1ΔL4 yielded high quality $^{1}H–^{15}N$ TROSY spectra in MSP1D1ΔH5 nanodiscs, confirming our interpretation of the origin of the non-uniform peak intensities in the spectra of the full-length protein. It should be possible in future experiments to further improve on these spectra and perform comprehensive structural studies on OprH with the shortened loops by including deuterated lipids into the MSP1D1ΔH5 nanodiscs.

The $^{1}H–^{15}N$ TROSY spectra that we obtained in $q = 0.3$ DHPC:DMPC:DHPS:DMPS bicelles were of superior quality compared to the spectra obtained in any of the nanodiscs, but not quite as good as those obtained in micelles. This effect cannot be explained only by differences in size, as the OprH bicelles molecular mass calculated from the 1D TRACT experiment was very similar to the predicted molecular mass of OprH in MSP1D1ΔH5 nanodiscs. The reason for this difference may be that the protein rotates faster in bicelles than in nanodiscs. This is plausible considering that bicelles contain much more detergent than nanodiscs and that the detergent is likely in rapid dynamical exchange with the protein perimeter. We also did not observe any adverse effect of bicelles on the stability of OprG and OprH. Both proteins remained stable in DHPC:DMPC:DHPS:DMPS bicelles over the course of several months, as they did in DHPC micelles. These bicelles are therefore good membrane mimetics for solution NMR studies of both proteins. The extent of secondary structure was almost identical for OprH in micelles and bicelles, but some HN chemical shifts, especially those near the membrane interfaces on the front side of the protein were different for OprH in the two environments. Somewhat different networks of dynamic hydrogen-bonding may explain these relatively subtle differences. Since more of these changes occur on one face than on the other face of the barrel, it is possible that the protein has a tendency to (transiently) dimerize in one environment but not the other. However, this interpretation is currently speculative and will need further experimental testing, which is beyond the scope of the present work.

In conclusion, it is clear that more extensive structural work by solution NMR is possible for two *Pseudomonas* β-barrel outer membrane proteins in lipid bicelles and promising but challenging in some of the smaller nanodiscs. The protein OprHΔL1ΔL4 with the shortened loops in MSP1D1ΔH5-DMPC nanodiscs is the most promising nanodisc sample at this stage. The quality of these spectra may be further improved in samples with deuterated lipids and by employing non-uniform NMR sampling methods (Rovnyak et al. 2004; Hyberts et al. 2013; 2014). This will make the collection of three-dimensional data sets and thorough structural studies of this protein in nanodiscs feasible.

Acknowledgments This work was supported by NIH grant R01 GM051329. We thank Dr. Tiandi Zhuang and members of the Tamm lab for numerous helpful discussions.

References

Bayburt TH, Grinkova YV, Sligar SG (2002) Single-molecule height measurements on microsomal cytochrome P450 in nanometer-scale phospholipid bilayer disks. Proc Natl Acad Sci U S A 99:6725–6730

Bocharov EV, Mayzel ML, Volynsky PE, Goncharuk MV, Ermolyuk YS, Schulga AA, Artemenko EO, Efremov RG, Arseniev AS (2008) Spatial structure and pH-dependent conformational diversity of dimeric transmembrane domain of the receptor tyrosine kinase EphA1. J Biol Chem 283:29385–29395

Delaglio F, Grzesiek S, Vuister GW, Zhu G, Pfeifer J, Bax A (1995) NMRPipe: a multidimensional spectral processing system based on UNIX pipes. J Biomol NMR 6:277–293

Denisov IG, Grinkova YV, Lazarides AA, Sligar SG (2004) Directed self-assembly of monodisperse phospholipid bilayer nanodiscs with controlled size. J Am Chem Soc 126:3477–3487

Edrington TC, Kintz E, Goldberg JB, Tamm LK (2011) Structural basis for the interaction of lipopolysaccharide with outer membrane protein H (OprH) from *Pseudomonas aeruginosa*. J Biol Chem 286:39211–39223

Ellena JF, Burnitz MC, Cafiso DS (2003) Location of the myristoylated alanine-rich C-kinase substrate (MARCKS) effector domain in negatively charged phospholipid bicelles. Biophys J 85:2442–2448

Etzkorn M, Raschle T, Hagn F, Gelev V, Rice AJ, Walz T, Wagner G (2013) Cell-free expressed bacteriorhodopsin in different soluble membrane mimetics: biophysical properties and NMR accessibility. Structure 21:394–401

Gluck JM, Wittlich M, Feuerstein S, Hoffmann S, Willbold D, Koenig BW (2009) Integral membrane proteins in nanodiscs can be studied by solution NMR spectroscopy. J Am Chem Soc 131:12060–12061

Goddard TD and Kneller DG SPARKY 3. University of California, San Francisco

Hagn F, Etzkorn M, Raschle T, Wagner G (2013) Optimized phospholipid bilayer nanodiscs facilitate high-resolution structure determination of membrane proteins. J Am Chem Soc 135:1919–1925

Hyberts SG, Arthanari H, Robson SA, Wagner G (2014) Perspectives in magnetic resonance: NMR in the post-FFT era. J Magn Reson 241:60–73

Hyberts SG, Robson SA, Wagner G (2013) Exploring signal-to-noise ratio and sensitivity in non-uniformly sampled multi-dimensional NMR spectra. J Biomol NMR 55:167–178

Lau TL, Partridge AW, Ginsberg MH, Ulmer TS (2008) Structure of the integrin beta3 transmembrane segment in phospholipid bicelles and detergent micelles. Biochemistry 47:4008–4016

Lee D, Hilty C, Wider G, Wuthrich K (2006) Effective rotational correlation times of proteins from NMR relaxation interference. J Magn Reson 178:72–76

Liang B, Dawidowski D, Ellena JF, Tamm LK, Cafiso DS (2014) The SNARE motif of synaptobrevin exhibits an aqueous-interfacial partitioning that is modulated by membrane curvature. Biochemistry 53:1485–1494

Linke D (2009) Detergents: an overview. Methods Enzymol 463:603–617

Losonczi JA, Prestegard JH (1998) Improved dilute bicelle solutions for high-resolution NMR of biological macromolecules. J Biomol NMR 12:447–451

Metzler WJ, Constantine KL, Friedrichs MS, Bell AJ, Ernst EG, Lavoie TB, Mueller L (1993) Characterization of the three-dimensional solution structure of human profilin: 1H, 13C, and 15 N NMR assignments and global folding pattern. Biochemistry 32:13818–13829

Mulder FA, Schipper D, Bott R, Boelens R (1999) Altered flexibility in the substrate-binding site of related native and engineered high-alkaline Bacillus subtilisins. J Mol Biol 292:111–123

Park SH, Berkamp S, Cook GA, Chan MK, Viadiu H, Opella SJ (2011) Nanodiscs versus macrodiscs for NMR of membrane proteins. Biochemistry 50:8983–8985

Poget SF, Cahill SM, Girvin ME (2007) Isotropic bicelles stabilize the functional form of a small multidrug-resistance pump for NMR structural studies. J Am Chem Soc 129:2432–2433

Raschle T, Hiller S, Yu TY, Rice AJ, Walz T, Wagner G (2009) Structural and functional characterization of the integral membrane protein VDAC-1 in lipid bilayer nanodiscs. J Am Chem Soc 131:17777–17779

Ritchie TK, Grinkova YV, Bayburt TH, Denisov IG, Zolnerciks JK, Atkins WM, Sligar SG (2009) Chapter 11—reconstitution of membrane proteins in phospholipid bilayer nanodiscs. Methods Enzymol 464:211–231

Rovnyak D, Frueh DP, Sastry M, Sun ZY, Stern AS, Hoch JC, Wagner G (2004) Accelerated acquisition of high resolution triple-resonance spectra using non-uniform sampling and maximum entropy reconstruction. J Magn Reson 170:15–21

Sanders CR 2nd, Prestegard JH (1990) Magnetically orientable phospholipid bilayers containing small amounts of a bile salt analogue, CHAPSO. Biophys J 58:447–460

Sanders CR, Prosser RS (1998) Bicelles: a model membrane system for all seasons? Structure 6:1227–1234

Sanders CR 2nd, Schwonek JP (1992) Characterization of magnetically orientable bilayers in mixtures of dihexanoylphosphatidylcholine and dimyristoylphosphatidylcholine by solid-state NMR. Biochemistry 31:8898–8905

Schuler MA, Denisov IG, Sligar SG (2013) Nanodiscs as a new tool to examine lipid-protein interactions. Methods Mol Biol 974:415–433

Song Y, Mittendorf KF, Lu Z, Sanders CR (2014) Impact of bilayer lipid composition on the structure and topology of the transmembrane amyloid precursor C99 protein. J Am Chem Soc 136:4093–4096

Struppe J, Komives EA, Taylor SS, Vold RR (1998) 2H NMR studies of a myristoylated peptide in neutral and acidic phospholipid bicelles. Biochemistry 37:15523–15527

Susac L, Horst R, Wuthrich K (2014) Solution-NMR characterization of outer-membrane protein A from *E. coli* in lipid bilayer nanodiscs and detergent micelles. ChemBioChem 15:995–1000

Tate CG (2010) Practical considerations of membrane protein instability during purification and crystallisation. Methods Mol Biol 601:187–203

Touw DS, Patel DR, van den Berg B (2010) The crystal structure of OprG from *Pseudomonas aeruginosa*, a potential channel for transport of hydrophobic molecules across the outer membrane. PLoS ONE 5:e15016

Tropea JE, Cherry S, Waugh DS (2009) Expression and purification of soluble His(6)-tagged TEV protease. Methods Mol Biol 498:297–307

Tzitzilonis C, Eichmann C, Maslennikov I, Choe S, Riek R (2013) Detergent/nanodisc screening for high-resolution NMR studies of an integral membrane protein containing a cytoplasmic domain. PLoS One 8:e54378

Wallin E, von Heijne G (1998) Genome-wide analysis of integral membrane proteins from eubacterial, archaean, and eukaryotic organisms. Protein Sci 7:1029–1038

Yu TY, Raschle T, Hiller S, Wagner G (2012) Solution NMR spectroscopic characterization of human VDAC-2 in detergent micelles and lipid bilayer nanodiscs. Biochim Biophys Acta 1818:1562–1569